Beam Profile Monitors for Emittance measurements

Kay Wittenburg, -DESY-

Transport lines and Linacs	Hadron accelerators	Electron accelerators
Phosphor Screens SEM Grids/Harps OTR Wire scanners (Linacs)	Wire scanners Residual Gas Ionization Residual Gas Scintillation Synchrotron light (Edge effect, wigglers) Scrapers/current (destructive)	Synchrotron light Wire Scanners Scrapers/current (destructive) Laser Wire Scanner
Emittance of single shots	Emittance preservation	Aspect ratio/coupling

Idea of this course: Beam Profile monitors use quite a lot of different physical effects to measure the beam size. Many effects on the beam and on the monitor have to be studied before a decision for a type of monitor can be made. In this session we will discuss emittance measurements and we will make some detailed examinations of at least two monitor types to demonstrate the wide range of physics of the profile instruments.

Synchrotron light profile monitor

In electron accelerators the effect of synchrotron radiation (SR) can be used for beam size measurements. In this course we will focus on profile determination, but SR can also be used for bunch length measurements with e.g. streak cameras with a resolution of < 1 ps. From classical electrodynamics the radiated power is given for a momentum change dp/dt and a particle with mass m_0 and charge e:

$$P_{SR} = \frac{e^2 c}{6\pi\varepsilon_0 (m_0 c^2)} \left[\frac{dp}{dt}\right]^2$$

For linear accelerators dp/dt = dW/dx. For typical values of dW/dx = 10 - 20 MeV/m the SR is negligible. In circular machines an acceleration perpendicular to the velocity exists mainly in the dipole magnets (field B) with a bending radius $\rho = \beta\gamma m_0 c/(eB)$. The total power of N circulating particles with $\gamma = E/m_0c^2$ is than

$$P_{tot} = \frac{e^2 c \gamma^4}{6\pi\varepsilon_0 \rho^2} N$$

This expression is also valid for a ring having all magnets of the same strength and field-free sections in between.

The critical wavelength λ_c divides the Spectrum of SR in two parts of equal power:

$$\lambda_c = \frac{4\pi\rho}{3\gamma^3}$$

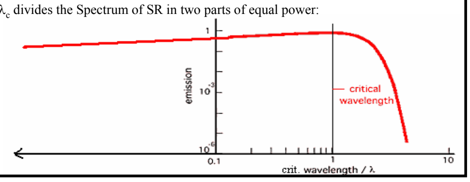

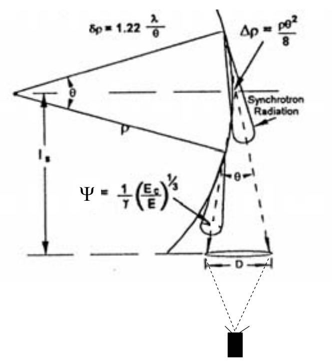

Opening angle Ψ of SR (1/2 of cone!) for $\lambda >> \lambda_c$:
with

$$\Psi = \frac{1}{\gamma}\left(\frac{\lambda}{\lambda_c}\right)^{1/3} = \left(\frac{3\lambda}{4\pi\rho}\right)^{1/3}$$

$\gamma = E/m_0c^2 = E$ [MeV]/0.511
$\gamma = 23483$ at 12 GeV and
$\gamma = 52838$ at 27 GeV
Path length s:
$s = \rho\theta$
ρ = Bending radius of Dipole

Example HERAe

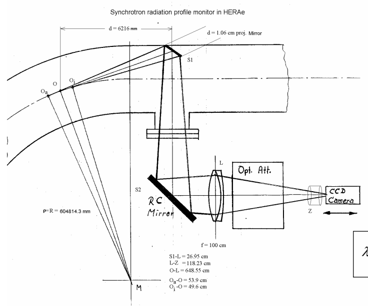

R = ρ = 604814.3 mm
G = O-L = 6485.5 mm
B = L-Z = 1182.3 mm
O-S1 = 6216 mm
L = O_a-O_i = 1035 mm
opening angle (horizontal): tanθ/2 = d/2/6216 => θ/2 = arc tan d/2/6216 = 0.85 mrad
opening angle (vertikal):
$\Psi(\lambda) = 1/\gamma\,(\lambda/\lambda_c)^{1/3}$

$$\lambda_c = \frac{4\pi\rho}{3\gamma^3} = 0.017\,nm < \lambda_c < 0.19\,nm$$

Exercise SR1 : Which problems with the setup can be expected?:

Heating of mirror:
⇒total emitted Power per electron:

$$P = \frac{e^2 c \gamma^4}{6\pi\varepsilon_0 \rho^2}$$

total Power of 46 mA circulating electrons at 27 GeV (Number of electrons $N_e = 6 \cdot 10^{12}$)

$\mathbf{P_{tot} = 6 \cdot 10^6}$ **W**

The mirror will get P_{tot} * Θ / (2 π) = **1600 W** (Integral over all wavelength!!!)
=> mirror is moveable, mirror has to be cooled
⇒ Material with low Z is nearly not visible for short wavelength => Beryllium
⇒ Still 100 W on mirror in HERAe

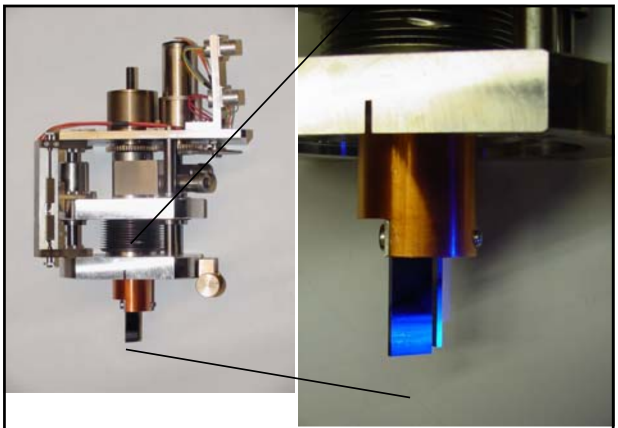

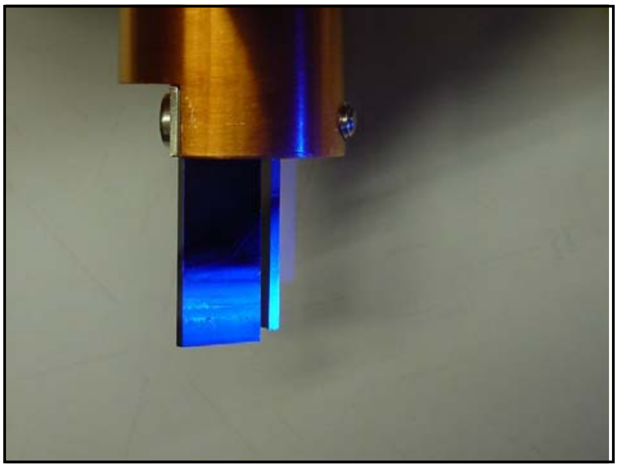

Exercise SR2: What limits the spatial resolution?

Diffraction, depth of field, arc, camera	=> physical
Alignment, lenses, mirrors, vibrations	=> technical

How to calibrate the optics?

Grid (yardstick) at point of emission, orbit bumps, …

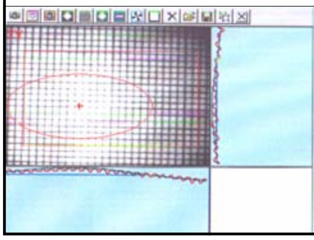

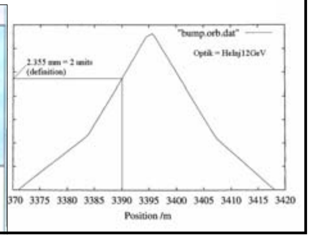

Diffraction:

EQ 1:
Diffraction limit (for Object):
For normal slit:
$\sigma_{Diff} = 0.47 * \lambda/\theta/2$ (horizontal, mirror defines opening angle θ)
$\sigma_{Diff} \approx 0.47 * \lambda/\Psi$ (vertikal)

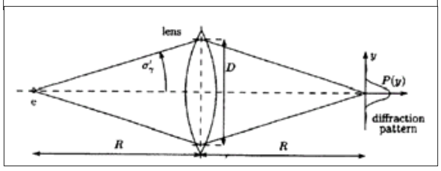

Depth of field:

EQ 2:
depth of field:
Vertical: $\Delta_{depth} \approx L/2 * \Psi = \sigma_{depth}$
Horizontal: $\Delta_{depth} \approx L/2 * \theta/2 = \sigma_{depth}$ (mirror defines opening angle θ)
$L \approx \rho \tan\theta$ or $2\rho\,(\theta/2 + \Psi)$

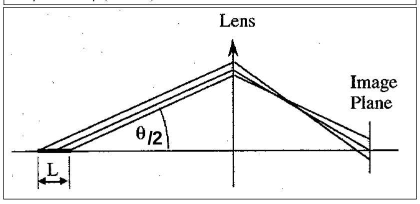

Arc:

EQ 3:
Arc (horizontal):
Observation of the beam in the horizontal plane is complicated by the fact that the light is emitted by all points along the arc. The horizontal width of the apparent source is related to the observation angle as:

$\Delta x_{arc} = \rho\,\theta^2/8 = \sigma_{arc}$ (mirror defines opening angle θ)

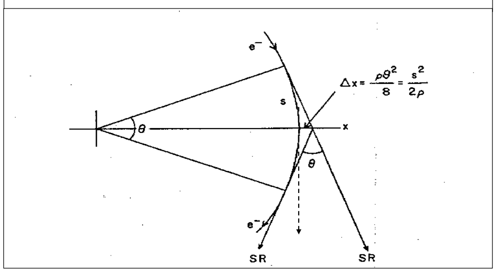

Camera (finite pixel size)

EQ 4:
Camera:
image gain = G/B = 5.485
typical resolution of camera CCD chip: $\sigma_{chip} = 6.7\ \mu m$
$\sigma_{camera} = \sigma_{chip} * G/B = 37\ \mu m$

Resolution:

λ not monochromatic !

$\sigma_{Diff} =$	$0.47 * \lambda/\theta$ (horizontal)	= ??? Depends on wavelength
$\sigma_{Diff} =$	$0.47 * \lambda/\Psi$ (vertikal)	= ??? Depends on wavelength
$\sigma_{depth} =$	$L/2 * \theta/2$	= 440 µm
$\sigma_{arc} =$	$\rho\,\theta^2/8$	= 219 µm (horizontal)
$\sigma_{camera} =$	$\sigma_{chip} * G/B$	= 37 µm

typical spectral sensitivities from CCD Sensors:

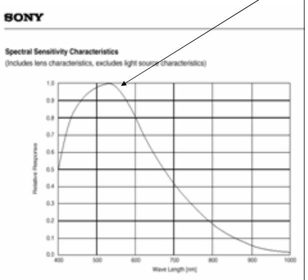

Assume: λ = 550 nm;
($\gamma = E/m_0c^2$)
$\gamma_{12} = 2.35 * 10^4$ (E = 12 GeV)
$\gamma_{35} = 6.85 * 10^4$ (E = 35 GeV)
$\lambda_{c,12} = (4\pi\rho)/(3\gamma^3) = 0.195$ nm at 12 GeV
$\lambda_{c,35} = (4\pi\rho)/(3\gamma^3) = 0.008$ nm at 35 GeV

opening angle (horizontal): $\tan\theta/2 = d/2/6216$ =>
$\theta/2 =$ arc tan d/2/6216 = 0.85 mrad

opening angle (vertikal):
$\Psi(\lambda) = 1/\gamma\,(\lambda/\lambda_c)^{1/3} = [(3\lambda)/(4\pi\rho)]^{1/3} = 0.6$ mrad

(mirror has to be larger than spot size on mirror) =>

σ_{diff} (horizontal)	$= 0.47 * \lambda/\theta/2$	= 304 µm
σ_{diff} (vertical)	$= 0.47 * \lambda/\Psi$	= 431 µm
σ_{depth}	$= L/2 * \theta/2$	= 440 µm
σ_{arc} (horizontal)	$= \rho\,\theta^2/8$	= 219 µm
σ_{camera}	$= \sigma_{chip} * G/B$	= 37 µm

$\sigma_{cor} = (\sigma_{diff}^2 + \sigma_{depth}^2 + \sigma_{arc}^2 + \sigma_{camera}^2)^{1/2}$ = 579 µm ; (horizontal)
$\sigma_{cor} = (\sigma_{diff}^2 + \sigma_{depth}^2 + \sigma_{camera}^2)^{1/2}$ = 617 µm ; (vertical)

Horizontal:
$\sigma_{cor} = [(\rho\,\theta^2/8)^2 + (L/2 * \theta/2)^2 + (0.47 * \lambda/\theta/2)^2]^{1/2}$
with $L \approx \rho \tan\theta \approx \rho\,\theta$

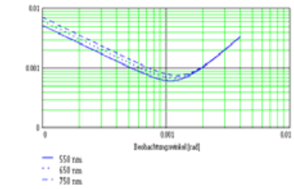

Vertical:
$\sigma_{cor} = [(L/2 * \Psi)^2 + (0.47 * \lambda/\Psi)^2]^{1/2}$ with
$L \approx \rho \tan\theta \approx \rho\,\theta$

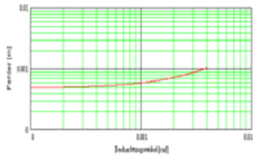

Not the whole truth:

1) Diffraction:

a) Ψ_{exact} is larger than the Gauss approximation (e.g. 0.79 → 1.08 mrad at Tristan)

b) For a gaussian beam the diffraction width is $\sigma_{diff} \approx 1/\pi * \lambda/\Psi$

(Ref: **ON OPTICAL RESOLUTION OF BEAM SIZE MEASUREMENTS BY MEANS OF SYNCHROTRON RADIATION**. By A. Ogata (KEK, Tsukuba). 1991. Published in Nucl.Instrum.Meth.A301:596-598,1991)

=> $\sigma_{diff} \approx 1/\pi * \lambda/\Psi_{exact}$ = 218 µm (Ψ_{exact} = 0.8 mrad, λ = 550 nm) vertical

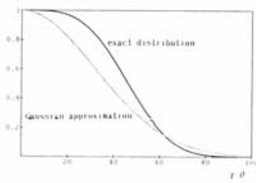

Fig. 1 Angular distribution of the 500 nm component of the synchrotron radiation from the TRISTAN MR bending magnet (246 m bending radius) operated at 30 GeV, and its Gaussian approximation.

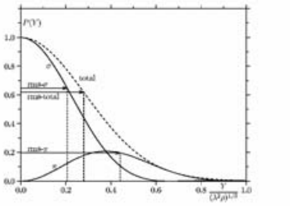

8: Fraunhofer diffraction for synchrotron radiation from long magnets

2) Depth of field:
The formula $R_{depth} = L/2 * \theta/2$ describes the radius of the distribution due to the depth of field effect. It is not gaussian and has long tails. The resolution of an image is probably much better than the formula above. A gaussian approximation with the same integral is shown in the figure below resulting in a width of σ_{depth} = 61 µm.

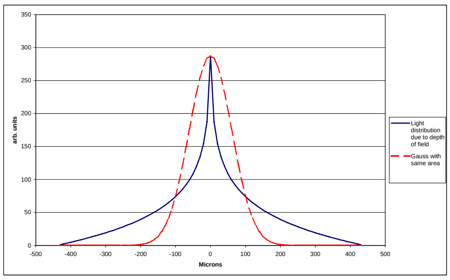

σ_{diff}	$= 0.47 * \lambda/\theta/2$	= 304 µm (horizontal)	before:
σ_{diff}	$= 1/\pi * \lambda/\Psi$	= 218 µm (vertical)	(431 µm)
σ_{depth}	$= L/2 * \theta/2$	= 61 µm	(440 µm)
σ_{arc}	$= \rho\,\theta^2/8$	= 219 µm (horizontal)	
σ_{camera}	$= \sigma_{chip} * G/B$	= 37 µm	

$\sigma_{cor} = (\sigma_{diff}^2 + \sigma_{depth}^2 + \sigma_{arc}^2 + \sigma_{camera}^2)^{1/2}$ = 381 µm ; (horizontal) (579 µm)
$\sigma_{cor} = (\sigma_{diff}^2 + \sigma_{depth}^2 + \sigma_{camera}^2)^{1/2}$ = 229 µm ; (vertical) (617 µm)

Beam width $\sigma_{beam} = (\sigma_{fit\_measured}^2 - \sigma_{cor}^2)^{1/2}$

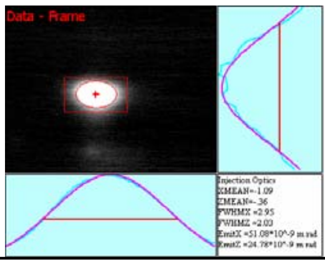

Exercise SR3: Discuss possible improvements of an SR-monitor:

- Monochromator at shorter wavelength (x-rays, need special optic)
- Use optimum readout angle
- Polarization - filter
- Use x-ray (λ < 0.1 nm) (LEP)

More:
Interferometer
The principle of measurement of the profile of an object by means of **spatial coherency** was first proposed by H.Fizeau and is now known as the Van Cittert-Zernike theorem. It is well known that A.A. Michelson measured the angular dimension (extent) of a star with this method.

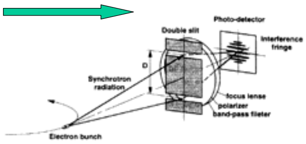

Referenzes
SPATIAL COHERENCY OF THE SYNCHROTRON RADIATION AT THE VISIBLE LIGHT REGION AND ITS APPLICATION FOR THE ELECTRON BEAM PROFILE MEASUREMENT.
By T. Mitsuhashi (KEK, Tsukuba). KEK-PREPRINT-97-56, May 1997. 4pp. Talk given at 17th IEEE Particle Accelerator Conference (PAC 97): Accelerator Science, Technology and Applications, Vancouver, Canada, 12-16 May 1997.

Intensity Interferometer and its application to Beam Diagnostics, Elfim Gluskin, ANL, publ. PAC 1991 San Francisco

MEASUREMENT OF SMALL TRANSVERSE BEAM SIZE USING INTERFEROMETRY
T. Mitsuhashi
High Energy Accelerator Research Organisation, Oho, Tsukuba, Ibaraki, 305-0801 Japan
DIPAC 2001 Proceedings - ESRF, Grenoble

Imaging: Compound Refractive Lens

lens-maker formula: $1/f = 2(n-1) / R$

X-ray refraction index : $n = 1 - \delta + i\beta, \quad \delta \approx 10^{-6}$

- concave lens shape
- strong surface bending R

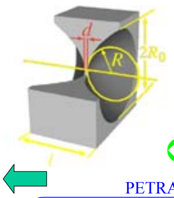

- small Z (Be, Al, …)
- small d

$f = \frac{R}{2\delta N}$

many lenses

courtesy of Ch. Schroer, TU Dresden

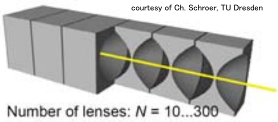

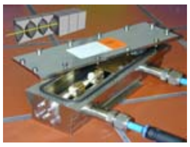

www.xray-lens.de

PETRA III @ 15 keV:

- R = 201.8 µm, R_0 = 447 µm, d = 10 µm
- N = 20
- material: beryllium

$f = 3.33\,\mathrm{m}$

$\sigma_{res} \approx 1\,\mu\mathrm{m}$

Interference: ATF (KEK)

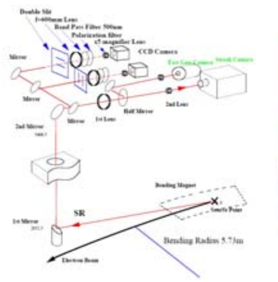

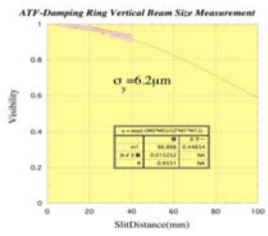

H.Hanyo et al., Proc. of PAC99 (1999), 2143

courtesy of T.Mitsuhashi, KEK

- smallest result: 4.7 µm with 400nm @ ATF, KEK

accuracy ~ 1 µm

Back to an imaging SR-Monitor: Still not the whole truth:

(Diffraction Limited) Resolution

Liénard-Wiechert potentials: $\varphi(t) = \left[\frac{-e}{R(1-\hat{n}\cdot\vec{\beta})}\right]_{ret}, \quad \vec{A}(t) = \left[\frac{-e\vec{\beta}}{R(1-\hat{n}\cdot\vec{\beta})}\right]_{ret}$

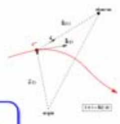

Liénard-Wiechert fields:

$\vec{E}(t) = -e\left(\frac{(1-\beta^2)(\hat{n}-\vec{\beta})}{R^2(1-\hat{n}\cdot\vec{\beta})^3} + \frac{\hat{n}\times[(\hat{n}-\vec{\beta})\times\dot{\vec{\beta}}]}{cR(1-\hat{n}\cdot\vec{\beta})^3}\right)_{ret}$

$\vec{B}(t) = \hat{n}\times\vec{E}(t)$

Fourier transform:

$\varphi_\omega = -e\int \frac{1}{R(\tau)} e^{i\omega(\tau+R(\tau)/c)} d\tau$

$\vec{A}_\omega = -e\int \frac{\vec{\beta}(\tau)}{R(\tau)} e^{i\omega(\tau+R(\tau)/c)} d\tau$

Fourier transform:

$\vec{E}_\omega \approx -\frac{ie\omega}{cR}\int [\hat{n}\times[\hat{n}\times\vec{\beta}]]\, e^{i\omega(\tau+R(\tau)/c)} d\tau$

Electric field:

$\vec{E}_\omega = -\frac{i\omega e}{c}\int \left[\frac{\vec{\beta}-\hat{n}}{R(\tau)} - \frac{ic}{\omega}\frac{\hat{n}}{R^2(\tau)}\right] e^{i\omega(\tau+R(\tau)/c)} d\tau$

point charge on circular orbit
→ analytical far field expressions for E_σ, E_π

numerical near field calculation depending on field geometry
→ free codes available (SRW, SPECTRA, …)

propagation in frame of scalar diffraction theory

$E_{\omega\perp,2} = -i\frac{\omega}{2\pi c}\int\int_\Sigma \frac{E_{\omega\perp,1}}{\rho}\exp[i\omega/c\,\rho]\,d\Sigma$

spectral flux density

$\frac{d^2 N_\omega}{d A\, d\omega/\omega} = \frac{\alpha c^2}{4\pi^2 e^2}|E_{\omega\perp,2}|^2$

Numerical way
Includes real electron path (depth of field and curve)

Classical way:
approximation

- Fraunhofer diffraction pattern for spherical wave
  → depth of field, orbit curvature: additional contributions
- accounts for the fact that SR is not actually a sporical wave
  → depth of field and orbit curvature included

A. Hofmann and F. Méot, Nucl. Instr. Meth. 203 (1982) 483

O. Chubar and P. Elleaume, Proceedings of the EPAC98, Stockholm, Sweden (1998) 1177

Resolution Broadening Effects for the HERAe Emittance Monitor

determination:

- calculation of spatial SR intensity distribution including beam emittance
- quadratical subtraction of beam size

For ∞ mirror size

horizontal profile

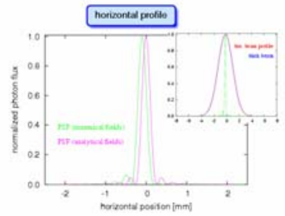

vertical profile

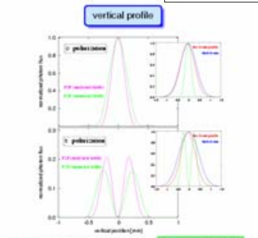

- broadening contribution: σ_{res} = 203 µm — numerical — broadening contribution: σ_{res} = 138 µm
- $\sigma_{diffract}$ = 188 µm, $\sigma_{dof+curv}$ = 275 µm → σ_{res} = 333 µm — analytical — $\sigma_{diffract}$ = 106 µm, σ_{dof} = 134 µm → σ_{res} = 171 µm

579 ->381-> 203 µm

617-> 229 -> 138 µm

- G. Kube, R. Fischer, K. Wittenburg, in Proceedings of BIW2004, AIP Conf. Proc. 732 (2004), p.350-357
- G. Kube, R. Fischer, Ch. Wiebers, K. Wittenburg, in Proceedings of DIPAC2005 (in press)

Vertical Resolution for Off-Axis Observation at HERAe

motivation:
- high heat load of extraction mirror
- opening angle Ψ_c for optical SR larger than for X-rays → x-ray miss the mirror

solution:
- observation in off-axis geometry ($y_m \geq 0$)

consequence:
- modification of lower bound in Kirchhoff integral (SR propagation through optical system)
  → additional resolution broadening

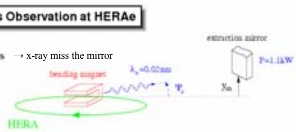

point spread function

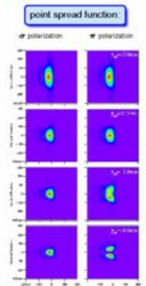

comparison

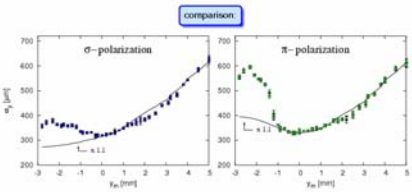

G. Kube, R. Fischer, K. Wittenburg, in Proceedings of BIW2004, AIP Conf. Proc. 732 (2004), p.350-357

G. Kube, R. Fischer, Ch. Wiebers, K. Wittenburg, in Proceedings of DIPAC2005 (in press)

Comparison SR-monitor vs Wire scanner

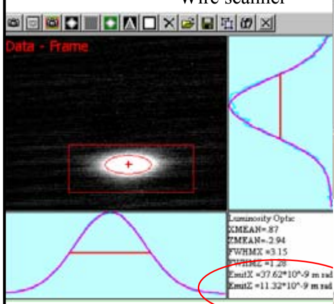

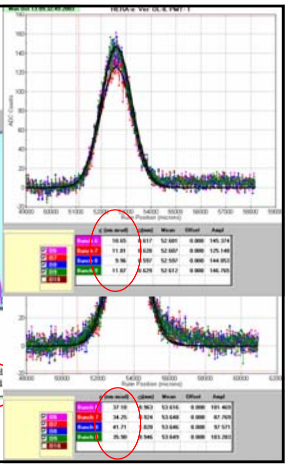

σ_y = 542 µm

Correction: 617-> 229 -> 138 µm

Proton Synchrotron Radiation Diagnostics

"Frequency Boost" of Synchrotron Radiation

task: production of sufficient synchrotron radiation intensity at high frequencies $\omega \gg \omega_c$

$\hookrightarrow$ intensity: $\boxed{\frac{d^2W}{d\Omega \frac{d\omega}{\omega}} \propto |\vec{E}_\omega|^2}$ with $\vec{E}_\omega = \frac{1}{\sqrt{2\pi}} \int_{-\infty}^{+\infty} dt\, \vec{E}(t)\, e^{i\omega t}$

intuitive approach: synchrotron radiation in time domain

1.) field shape for on-axis observation (i.e. $E_\psi = 0$)

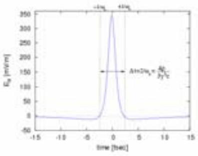

2.) pulse length estimation at fixed observation point

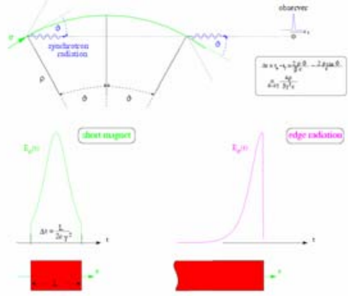

truncation of wave train:

- R. Coïsson, Phys. Rev. **A 20** (1979) 524
- F. Méot, Particle Accelerators **62** (1979) 215
- A. Hofmann, CAS proceedings 98-04

Generation of Frequency Boost

sharp cut-off of wavetrain in time domain

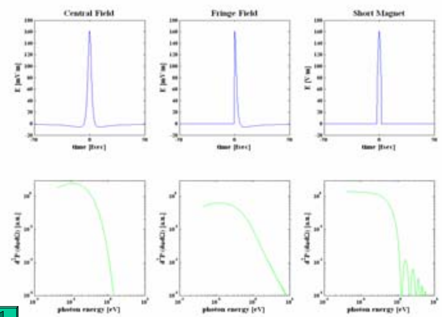

$\Uparrow$

$$\frac{d^2N}{d\Omega d\omega/\omega} \propto |\vec{E}_\omega|^2$$

with

$$\vec{E}_\omega = \frac{1}{\sqrt{2\pi}} \int_{-\infty}^{+\infty} dt\, \vec{E}(t) e^{i\omega t}$$

still requires high beam energies (CERN, Tevatron, HERA)

Wire Scanners

Introduction

Conventional wire scanners with thin solid wires (conventional compared with new techniques using, for example, Lasers) are widely used for beam size measurements in particle accelerators.

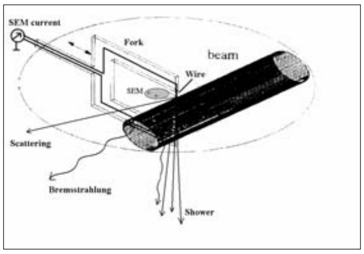

Their advantages:

1) Resolution of down to 1 μm
2) Trusty, reliable
3) Direct

0.1 micron position resolution is possible

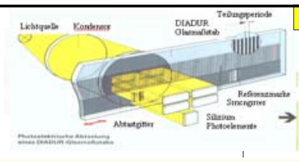

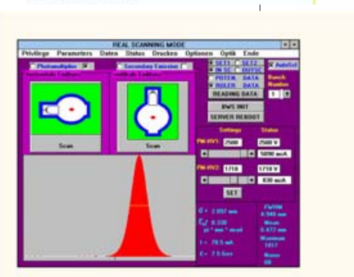

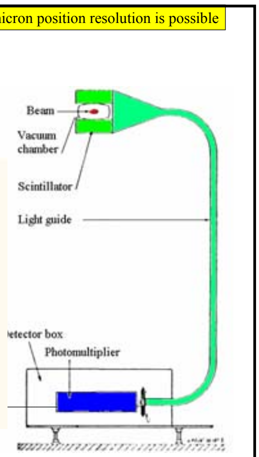

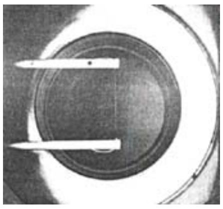

CERN/DESY 1990-2003

Speed: 1 m/s
Scanning area: approx. 10 cm
Wire material: Carbon/Quartz
Wire diameter: 7 microns
Signal: shower

1 micron resolution

Where one should locate the Scintillator?

Projected angular distribution could be approximated by Gaussian with a width given by

$$\Theta_{mean} = \frac{0.014GeV}{pc} \cdot \sqrt{\frac{d'}{L_{rad}}} \cdot \left(1 + 1/9 \cdot \log_{10} \frac{d'}{L_{rad}}\right)$$

d' = 1.5×10^{-3} cm – the thickness of the target, X_0=12.3 cm – quartz-wire radiation length, x/X_0 = 1.22×10^{-4}
It is corresponding to:

$$\Theta_{mean} \approx 3.0\times10\text{-}6 \text{ rad}$$

for electron momentum of 30GeV/c.

Scattered particles will arrive vacuum chamber of radius R = 2 cm at:

$$z \approx \frac{R}{\Theta_{mean}\sqrt{2}} \approx 4.9km!!!!$$

What to do?

Monte Carlo simulations of best location for scintillators

Protons at 920 GeV/c

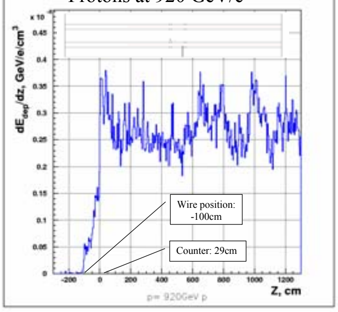

Electrons at 30 GeV/c

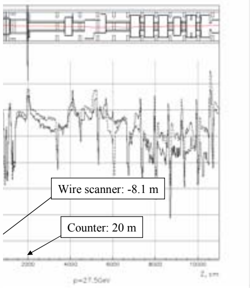

Simulation includes all magnetic fields
as well as all elastic and inelastic scattering cross sections

Wire scanner's known limitations are:

1. The smallest measurable beam size is limited by the finite wire diameter of a few microns,
2. Higher Order Modes may couple to conductive wires and can destroy them,
3. High beam intensities combined with small beam sizes will destroy the wire due to the high heat load.
4. Emittance blow up

Limitations:

1. Wire size
The smallest achievable wires have a diameter of about 5-6 µm.
An example of the error in the beam width determination is shown for a 36 µm wire.

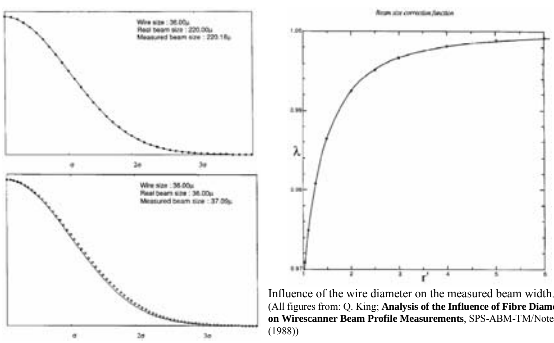

Influence of the wire diameter on the measured beam width.
(All figures from: Q. King; **Analysis of the Influence of Fibre Diameter on Wirescanner Beam Profile Measurements**, SPS-ABM-TM/Note/8802 (1988))

Limitations:

2. Higher Order modes
An early observation (1972 DORIS) with wire scanners in electron accelerators was, that the wire was always broken, even without moving the scanner into the beam. An explanation was that Higher Order Modes (HOM) were coupled into the cavity of the vacuum chamber extension housing the wire scanner fork. The wire absorbs part of the RF which led to strong RF heating.

Exercise WIRE1: Discuss methods of proving this behavior. What are possible solutions against the RF coupling?

Methods:
1. Measurement of wire resistivity
2. Measurement of thermo-ionic emission
3. Optical observation of glowing wire
4. Measurement of RF coupling in Laboratory with spectrum analyzer

1. Measurement of wire resistivity

The wire resistivity will change depending on the temperature of the wire, even without scanning.

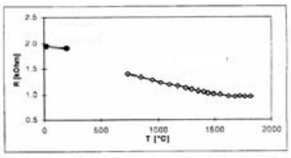

Fig 4: Measured wire resistance variations with temperature.

Here: 8 µm Carbon wire
(from OBSERVATION OF THERMAL EFFECTS ON THE LEP WIRE SCANNERS. By J. Camas, C. Fischer, J.J. Gras, R. Jung, J. Koopman (CERN). CERN-SL-95-20-BI, May 1995. 4pp. Presented at the 16th Particle Accelerator Conference - PAC 95, Dallas, TX, USA, 1 - 5 May 1995. Published in IEEE PAC 1995:2649-2651)

2. Measurement of thermo-ionic emission

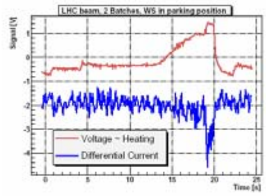

Wire heating due to the LHC beam injection in the SPS (No scan, wire in parking position).
The beam energy ramp/bunch length decreasing begin t=11 s.

A constant current was supplied to the wire and the voltage drop across it was fed to a digital scope together with the difference between the input and output currents. The differential current (I_{out}-I_{in}) grow up is due to the wire heating and consequent emission of electrons for thermionic effect. Fig. WIRE5 shows such voltage and differential current evolutions during the SPS cycle with LHC type beam. No scans were performed along this cycle. It is thus evident that the wire heating does not depend on the direct wire-beam interaction only.
(From **CAVITY MODE RELATED WIRE BREAKING OF THE SPS WIRE SCANNERS AND LOSS MEASUREMENTS OF WIRE MATERIALS**
F. Caspers, B. Dehning, E.Jensen, J. Koopman, J.F. Malo, CERN, Geneva, Switzerland
F. Roncarolo, CERN/University of Lausanne, Switzerland; DIPAC03)

3. Optical observation of glowing wire

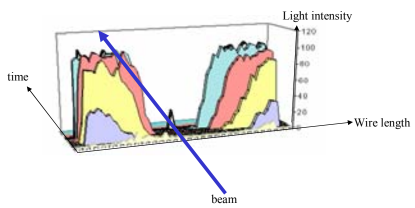

Digitized video recording of an 8 µm carbon wire scanning a 0.8 mA beam. The wire is parallel to the horizontal axis, and the light intensity is plotted along the vertical axis (arbitrary units). Successive profiles are separated by 20 ms. The central spot corresponds to the passage of the wire through the beam. Thus, RF heating led to (huge) thermal glowing before the beam interacts with the wire.
(from: QUARTZ WIRES VERSUS CARBON FIBERS FOR IMPROVED BEAM HANDLING CAPACITY OF THE LEP WIRE SCANNERS.
By C. Fischer, R. Jung, J. Koopman (CERN). CERN-SL-96-09-BI, May 1996. 8pp. Talk given at 7th Beam Instrumentation Workshop (BIW 96), Argonne, IL, 6-9 May 1996.

4. Measurement of RF coupling with spectrum analyzer

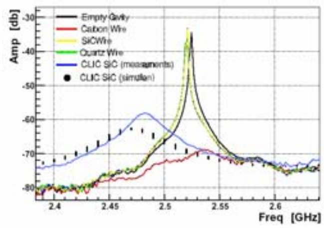

Resonant cavity signal in presence of Carbon (36 µm), Silicon Carbide and Quartz wires

The plot qualitatively proves the RF power absorption of Carbon, and the non-absorption of Silicon Carbide and Quartz. Absorbed energy is mainly converted into heat.

What are solutions for the problems 1-4?

Damping of Higher Order Modes with Ferrites etc.
Non conducting wires

Limitations:

3. Wire heat load
According to Bethe-Blochs formula, a fraction of energy dE/dx of high energy particles crossing the wire is deposit in the wire. Each beam particle which crosses the wire deposits energy inside the wire. The energy loss is defined by dE/dx (minimum ionization loss) and is taken to be that for a minimum ionizing particle. In this case the temperature increase of the wire can be calculated by:

unknown

$$T = C \cdot dE/dx_m \cdot d' \cdot N \cdot \frac{1}{c_p \cdot G} \quad [{}^0C]$$

where N is the number of particles hitting the wire during one scan, d' is the thickness of a quadratic wire with the same area as a round one and G [g] is the mass of the part of the wire interacting with the beam. The mass G is defined by the beam dimension in the direction of the wire (perpendicular to the measuring direction):

Parameter table

Exercise WIRE2: Which kind of wire Material you will prefer for a wire scanner in this accelerator?

Estimate the wire temperature after one scan with a speed v (assume no cooling mechanisms).

Solving G: G [g] is the mass of the part of the wire interacting with the beam. The mass G is defined by the beam dimension in the direction of the wire (perpendicular to the measuring direction) and by the wire diameter d':

$$\boxed{G = wire\ volume \cdot \rho = 2 \cdot \sigma_v \cdot d'^2 \cdot \rho \quad [g]}$$

Solving N:
The number of particles N hitting the wire during one scan depends on the speed of the scan (~1/v), the revolution frequency (~f_{rev}), the wire diameter (~d') and the beam current (~NB · n_{bunch}):

$$\boxed{N = \frac{d' \cdot f_{rev}}{v} \cdot (NB \cdot n_{bunch})}$$

The figure shows the a graphical representation of the parameters. The quotient d·f/v is the ratio of the scanned beam area or, in other words, like a grid seen by one bunch, assuming that all bunches are equal. However, the ratio can exceed the value 1 (a foil) if the scanning distance between two bunches is smaller than the wire diameter. Note that N does not depend on the beam widths σ.

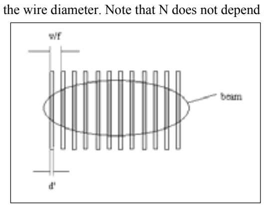

Geometrical meaning of the parameters v/f and d'

Therefore, the temperature increase of the wire after one scan becomes:

$$T = C \cdot dE/dx_m \cdot d' \cdot N \cdot \frac{1}{c_p \cdot G} \quad [^0C]$$

In MeV/cm

$$Mass\, G = wire\ volume \cdot \rho = 2 \cdot \sigma_v \cdot d'^2 \cdot \rho \quad [g]$$

$$N = \frac{d' \cdot f_{rev}}{v} \cdot (NB \cdot n_{bunch})$$

$$T_h = C \cdot dE/dx_m \cdot \cancel{d'} \cdot \frac{\cancel{d'} \cdot f_{rev}}{v} \cdot (NB \cdot n_{bunch}) \cdot \frac{1}{c_p \cdot 2 \cdot \sigma_v \cdot \cancel{d'^2} \cdot \rho} \cdot \alpha \quad [^0C]$$

$$with \quad \frac{dE/dx_m}{\rho} = dE/dx \left[\frac{MeV \cdot cm^2}{g}\right] \quad and \quad f_{rev} \cdot NB = f_{bunch}$$

$$\Downarrow$$

$$T_h = C \cdot dE/dx \cdot n_{bunch} \cdot \frac{f_{bunch}}{v} \cdot \frac{1}{c_p \cdot 2 \cdot \sigma_v} \cdot \alpha \quad [^0C]$$

Parameter table

Where h, denotes the horizontal (h) scanning direction. The cooling factor 'α' is described in the next section. **Note that the temperature does not depend on the wire diameter and that it depends on the beam dimension perpendicular to the measuring direction. The temperature increase is inverse proportional to the scanning speed**, therefore a faster scanner has a correspondingly smaller temperature increase.

The wire parameters dE/dx / cp and the Quotient Th/Tm should be minimal for a choice of the material (a = 1):

Material	$dE/dx / c_p$	T_h [^{0}C]	T_h/T_m
AL	7.7	$1.1 \cdot 10^4$	16.9
W	50.6	$7.1 \cdot 10^4$	20.9
C	5.4	$0.77 \cdot 10^4$	2.2
Be	4.1	$0.58 \cdot 10^4$	4.8
SiO2	12.9	$1.8 \cdot 10^4$	10.6

TableWire3: calculated Temperatures

From Table WIRE3 follows, that even the best material (Carbon) will be a Factor 2.2 above its melting temperature.

Small pit marks seen near the end of the wire are further evidence for arcing.

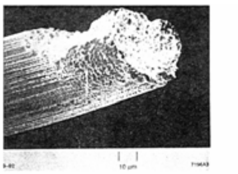

Figure 3. Electron microscope picture of a 40 µm tungsten wire break. This wire was installed in an SLC linac wire scanner.

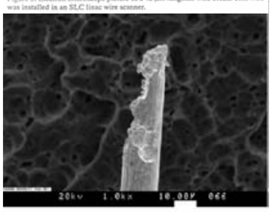

FIGURE 1. Failed 15 µm diameter tungsten wire showing the rough surface resulting from many discharges.

Burned by the e-beam at SLC

Exercise WIRE2a: Discuss cooling mechanisms which will cool the wire.

1) Secondary particles emitted from the wire
2) Heat transport along the wire
3) Black body radiation
4) Change of c_p with temperature

Wire type	Approximation Q (µJ)	Monte Carlo Q (µJ)
10 µm graphite	0.140	0.169 ± 0.002
10 µm tungsten	1.01	2.19 ± 0.04
15 µm tungsten	2.27	4.90 ± 0.05
50 µm tungsten	25.3	32.0 ± 0.1

Heat deposited in various wire types by a passing bunch of 1 nC. The approximated value follows (1), the "Monte Carlo" result is obtained by the simulation of an electromagnetic shower with Fluka.

Thermal Load on Wirescanners
Lars Fröhlich
37th ICFA Advanced Beam Dynamics Workshop on Future Light Sources; May 15-19, 2006 in Hamburg, Germany

1) Secondaries:
Some energy is lost from the wire by secondary particles. In the work in (J. Bosser et al.; The micron wire scanner at the SPS, CERN SPS/86-26 (MS) (1986)) about 70% is assumed. In DESY III (example above) no carbon wire was broken during more than 10 years of operation. At HERA, the theoretical temperature of the carbon wire (without secondaries) exceeds the melting temperature after a scan by far (T = 12800 ^{0}C). Considering the loss by secondaries of 70%, the temperature reaches nearly the melting point. In practice, the wire breaks about once in 2 months. The observation is that the wire becomes thinner at the beam center. This may indicate, that during a scan some material of the wire is emitted because of nuclear interactions or is vaporized because it is very close to the melting temperature. This supports the estimate of the 70% loss and one has to multiply the factor α = 0.3 in the equation above

2) Heat transport: The transport of heat along the wire does not contribute **to short time cooling** of the wire (P. Lefevre; CERN PS/DL/Note 78-8). However, frequent use of the scanner heats up also the ends of the wire and its connection to the wire holders (fork).
For low repetition rates (LINACs) this is the major cooling mechanism.

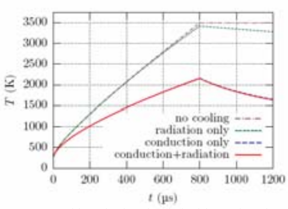

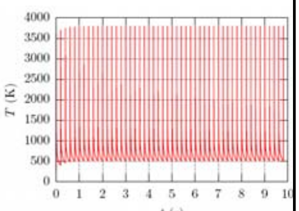

10 µm graphite wire bombarded with 800 bunches at 1 MHz; simulated with various combinations of cooling mechanisms, 5 Hz rep. rate.

Thermal Load on Wirescanners; Lars Fröhlich; 37th ICFA Advanced Beam Dynamics Workshop on Future Light Sources; May 15-19, 2006 in Hamburg, Germany

3) Black body radiation: The temperature T_{bb} at which the radiated power is equal to the deposited power in the wire during one scan P_{dep} [MeV/s] can be calculated from the Stefan-Bolzmann-law:

$$T_{bb} = \sqrt[4]{\frac{P_{dep}}{s \cdot A}}$$

where s = 35.4 MeV / (s^1 cm^2 $^0K^4$) is the Stefan-Bolzmann-constant and A is the area of radiating surface. The surface of the heated wire portion A is $2 \cdot \sigma_v \cdot d \cdot \pi$ [cm^2]. The power can be calculated by:

$$P_{dep\ h,v} = \alpha \cdot dE/dx \cdot d' \cdot n_{bunch} \cdot \frac{f_{bunch} \cdot d'}{v} \cdot \frac{1}{t_{scan}} \quad [MeV/s]$$

where $t_{scan} = 2 \cdot \sigma_{h,v} / v$ is the time for a scan (in the assumption of 2 σ it is neglected that only about 70% of the power is concentrated within 2 σ). α is the expected loss from secondaries.
For the example above T_{bb} = 3900 ^{0}C. **Therefore the black body radiation is only a fraction of cooling in case of fast scans.**

4) $c_p(T)$: The heat capacitance is a function of the temperature. Fig. 2 shows the increase of c_p for Carbon with T. The expected temperature after a scan is inversely proportional to c_p. **Therefore one can expect a slightly smaller resulting temperature because of this dependence.**

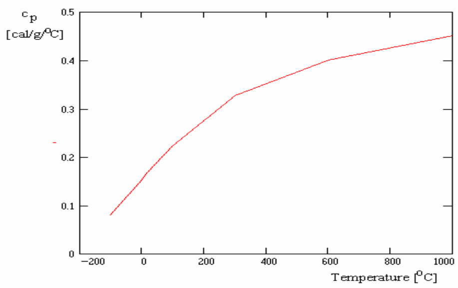

Temperature of the wire (v=1m/s)

	Num. of part.	Typ. Beam diam.	Temp. after scan [C]	Eqi. - Temp [Celsius]
HERAp	1 *10^13	0.7 mm	3900	5100
HERAe	6.5 * 10^12	0.2 mm	4800	4500
PETRAp	4.8*10^12	2 mm	980	3500
PETRAe	1.5*10^12	0.1 mm	4700	6800
DESYIII	1.2*10^12	1 mm	3400	5300
TTF fast	2.8*10^13	0.05 mm	4000	7400
TTF slow	2.8*10^13	0.05 mm	286 000	2900

Melting temperature = 3500 ºC for Carbon
= 1700 ºC for Quartz

The wire in DESY III still exists with 200 mA = $1.25 \cdot 10^{12}$ p
In HERA we exchange the wires every 2 month after "normal" use. Unusual frequent use will destroy the wires much earlier.

Limitations

Parameter table

4: Emittance blow up

Exercise WIRE3: Calculate the emittance blowup of the proton beam after one scan at a position with β = 11.8 m for p =0.3 and 7 GeV/c (Carbon wire):
Assume a measurement position close to a Quadrupole (α=0)

For small deflection angles a good approximation for average root mean square scattering angle is given by:

$$\delta\Theta = \frac{0.014\,GeV}{pc} \cdot \sqrt{\frac{d'}{L_{rad}}} \cdot \left(1 + 1/9 \cdot \log_{10}\frac{d'}{L_{rad}}\right)$$

Remember:
$\gamma(s)^2 y + 2\alpha(s) yy' + \beta(s) y'^2 = \varepsilon$

A fraction Ψ of the circulating beam particles will hit the wire:

$$\Psi = \frac{d' \cdot f_{rev}}{v}$$

(see exercise WIRE2)

The resulting emittance blowup is than:

$$\delta\,\varepsilon_{rms} = \sqrt{2\pi} \cdot \delta\Theta^2 \cdot \Psi^2 \cdot \beta$$
$$= 5.1 \cdot 10^{-2}\,\pi\,mm\,mrad$$

$\sqrt{2\pi}$ from Literature

Gas: emittance growth due to residual gas per hour ($P=10^{-9}$ mbar)

δε/ε [%/scan]

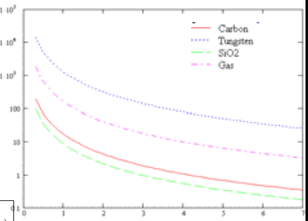

Momentum [GeV/c]

D. Möhl, Sources of emittance growth (also P. Bryant; CAS, Beam transfer lines):

$$\delta\varepsilon = \pi \frac{1}{2} \cdot \Theta_{rms}{}^2 \cdot \beta$$

Averaging over all Betatron-phases

Unit of phase space emittance

M. Giovannozzi (CAS 2005)

$$\delta\varepsilon = \pi \frac{1}{4} \cdot \Theta_{rms}{}^2 \cdot \beta$$

D. Möhl, Sources of emittance growth, 2007:

$$\delta\varepsilon_\sigma = \frac{1}{2} \cdot \Theta_{rms}{}^2 \cdot \beta$$

Wire Parameters

Parameter	Symbol	Unit	wire material				
			AL	W	Carbon	Beryllium	Quartz (SiO_2)
wire diameter	d $= 7 \cdot 10^{-4}$	cm					
mean wire diameter	$d' = d/2 \cdot \sqrt{\pi}$ $= 5.5 \cdot 10^{-4}$	cm					
Conversion	0.239	cal/Joule					
Conversion factor	$C = 3.8 \cdot 10^{-14}$	MeV / cal					
Speed of wire	v = 100	cm/s					
specific heat capacity*	c_p	cal / g / ^{0}C	0.21	0.036	0.42 (>400^{0}C) 0.17 (< 400^{0}C)	0.43	0.18
Energy loss of min. ion. part. (MIPs)	dE/dx dE/dx_m	MeV cm^2 / g MeV/cm	1.62 4.37	1.82 35.13	2.3 5.3	1.78 3.3	2.33 5.3
density	ρ	g/cm^3	2.7	19.3	2.3	1.85	2.29
melting temp.	T_m	^{0}C	650	3400	ca. 3500	1200	1700
Heat conductivity	l	W/(m K)	230	100-160	30-3000	200	1.2-1.4
Radiation length	l_{rad}	cm	8.9	0.35	18.8	34.7	12.3
Nuclear coll length	lnuc	cm	26	9.6	34	30	25.4

Table WIRE1: Parameters of wire materials. *> 500 ^{0}C

The beam parameters used in this exercise are shown in the following table:

Parameter	Symbol	Unit	Value
circumference of accel.	circ.	m	300
particle		Proton	
Beam particle momentum	p	GeV/c	0.3-7
Beta function	$\beta_h = \beta_v$	m	11.8
Emittance	$\varepsilon_h = \varepsilon_v$	π mm mrad	15
revolution Frequency	f_{rev}	MHz	0.93
Bunch spacing	t_{bunch} f_{bunch}	ns MHz	98 10.2
Number of bunches in accel.	NB		11
Bunch charge	n_{bunch}	1/e	$1.1 \cdot 10^{11}$
Beam width measurement [1]	σ_h	mm	1.5
Beam width perpendicular to meas. [1]	σ_v	mm	1

Table WIRE2: Parameters of Beam

LINACS/Transport Lines Emittance Measurement

In a transfer line, the beam passes once and the shape of the ellipse at the entry to the line determines its shape at the exit. Exactly the *same* transfer line/Linac injected first with one emittance ellipse and then different ellipses has to be accredited with *different* α and β, γ functions to describe the cases. **Thus α and β, γ depend on the input beam and their propagation depends on the structure.** Any change in the structure will only change the α and β, γ values downstream of that point. … The input ellipse must be chosen by the designer and should describe the configuration of all the particles in the beam.

In the following let's assume a transport line or the part of the Linac where no acceleration takes place. What about the emittance?

If no energy is transferred to the beam (Hamiltonian systems), the emittance is conserved.

Explain ways of measuring the emittance of a charged particle beam in a Linear Accelerator or a transport line without knowing the beam optic parameters α, β, γ.

Exercise L1: Which one is the preferable method for a high energy proton transport line (p > 5 GeV)?

Solution: 3 (thin) screens or SEM grids or varying quadrupole which measure the different beam widths σ. For pepper pot or slits one needs a full absorbing aperture.

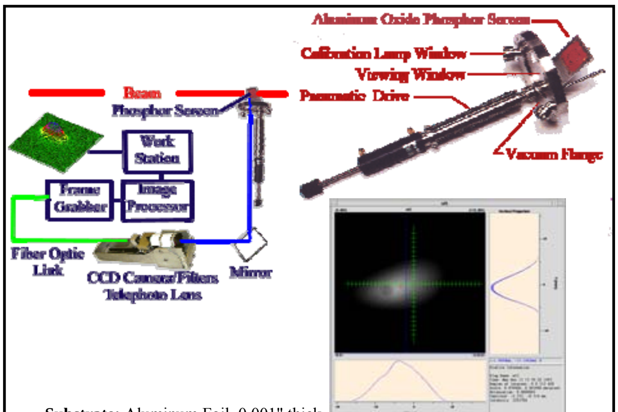

Substrate: Aluminum Foil, 0.001" thick

http://accelconf.web.cern.ch/AccelConf/p95/ARTICLES/TPB/TPB26.PDF

http://www.rhichome.bnl.gov/RHIC/Instrumentation/Systems/InjProfile/flags.html

Secondary Emission Dectectors

Introduction

When electrically charged particles with sufficient kinetic energy hit the surface of a solid, the latter emits electrons. These electrons are called *secondary* electrons, and the bombarding electrons are called *primary* electrons.

SE Grids

When a beam passes through a foil or a wire, a few percent of low energy electrons, with respect to the incoming particles, are emitted from the superficial layers. This charge depletion is proportional to the local density of the beam and can be used to measure a beam density profile.

The main problems encountered with these monitors are the small useful signal (pC) generated under a very high source impedance, and the collection of unwanted parasitic charges.

The monitors are, in general, built with the thinnest possible foils to minimize disturbance to the beam.

The main limitations of these monitors are their resolution, owing to the finite number and dimension of the strips, and the overall gain spread from channel to channel.

The resolution can be increased in single-shot operations by inclining the grid with respect to the beam direction. In a multi pulse measurement, the resolution can be increased by displacing the grid between measurements.

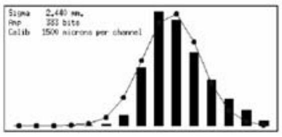

Measured profile and fitted gussian

http://sl-div-bi-pb.web.cern.ch/sl-div-bi-pb/Welcomesem.html

SEM grid with 15 foils to measure the beam profile. The large foils at either side of the grid are connected electrically together to form a 16-th channel.

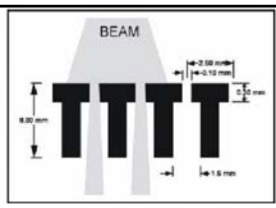

Scheme of the pepperpot plate in a cross sectional view and relevant dimensions

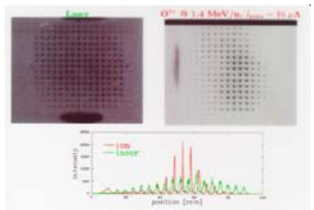

Light spots observed on the viewing screen of a Pepperpot device. Top left: Spots generated for calibration using a laser beam. Top right: Spots from an oxygen beam. Bottom: Intensity distribution along one line.

Three screen method:

If β is known unambiguously as in a circular machine, then a single profile measurement determines ε by

$$\sigma_y^2 = \varepsilon\beta_y.$$

But it is not easy to be sure in a transfer line which β to use, or rather, whether the beam that has been measured is matched to the β−values used for the line. This problem can be resolved by using three monitors (see Fig. 1), i.e. the three width measurement determines the three unknowns α, β and ε of the incoming beam.

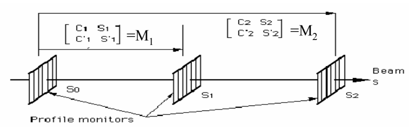

Exercise L2: Assuming that the geometry between the measurement stations and the transport matrices $M_{1,2}$ of the transport line are well defined (including magnetic elements), describe a way to get the emittance using the 3 screens and the σ−matrix.

Unfair, not introduced in the lessons, sorry

Introduction of σ-Matrix

(see for example: K. Wille; Physik der Teilchenbeschleuniger, Teubner)

$$\sigma = \begin{pmatrix} \sigma_{11} & \sigma_{12} \\ \sigma_{21} & \sigma_{22} \end{pmatrix} = \begin{pmatrix} \sigma_y^2 & \sigma_{yy'} \\ \sigma_{yy'} & \sigma_{y'}^2 \end{pmatrix} = \varepsilon_{rms} \begin{pmatrix} \beta & -\alpha \\ -\alpha & \gamma \end{pmatrix} = \sigma\, matrix$$

$$\boxed{\varepsilon_{rms} = \sqrt{\det\sigma} = \sqrt{\sigma_{11}\sigma_{22} - \sigma_{12}^2}} \qquad (\beta\gamma - \alpha^2 = 1)$$

Beam width_{rms} of measured profile = $\sigma_y = \sqrt{\beta(s)\cdot\varepsilon}$

Transformation of σ−Matrix through the elements of an accelerator:

$$\boxed{\sigma_s = M\cdot\sigma_0\cdot M^t} \qquad M = \begin{pmatrix} M_{11} & M_{12} \\ M_{21} & M_{22} \end{pmatrix};\ M^t = \begin{pmatrix} M_{11} & M_{21} \\ M_{12} & M_{22} \end{pmatrix}$$

L_1, L_2 = distances between screens or from Quadrupole to screen and Quadrupole field strength are given, therefore the transport matrix M is known.

Applying the transport matrix gives (now time for exercise):

Exercise L2: Assuming that the geometry between the measurement stations and the transport matrices M1,2 of the transport line are well defined (including magnetic elements), describe a way to get the emittance using the 3 screens and the s-matrix.

$$\boxed{\sigma_s = M \cdot \sigma_0 \cdot M^t}$$

$$= \begin{pmatrix} M_{11} & M_{12} \\ M_{21} & M_{22} \end{pmatrix} \cdot \begin{pmatrix} \sigma_{11} & \sigma_{12} \\ \sigma_{21} & \sigma_{22} \end{pmatrix} \cdot \begin{pmatrix} M_{11} & M_{21} \\ M_{12} & M_{22} \end{pmatrix} = \sigma^{measured} = \begin{pmatrix} \sigma_y^2 & \sigma_{yy'} \\ \sigma_{y'y} & \sigma_{y'}^2 \end{pmatrix}^{measured} = \varepsilon_{rms} \begin{pmatrix} \beta & -\alpha \\ -\alpha & \gamma \end{pmatrix}$$

$$= \begin{pmatrix} M_{11} & M_{12} \\ M_{21} & M_{22} \end{pmatrix} \cdot \begin{pmatrix} \sigma_{11}M_{11} + \sigma_{12}M_{12} & \sigma_{11}M_{21} + \sigma_{12}M_{22} \\ \sigma_{21}M_{11} + \sigma_{22}M_{12} & \sigma_{12}M_{21} + \sigma_{22}M_{22} \end{pmatrix}$$

$$= \begin{pmatrix} M_{11}(\sigma_{11}M_{11} + \sigma_{12}M_{12}) + M_{12}(\sigma_{21}M_{11} + \sigma_{22}M_{12}) & \cdots \\ \cdots & \cdots \end{pmatrix}$$

$$\sigma_{11}^{measured} = \sigma^{2\,measured}_y = M_{11}^2\sigma_{11} + 2M_{11}M_{12}\sigma_{12} + M_{12}^2\sigma_{22} \quad (\sigma_{12} = \sigma_{21}) \qquad (1)$$

Solving σ_{11} σ_{12} and σ_{22} while Matrix elements are known: Needs minimum of three different measurements, either three screens or three different Quadrupole settings with different field strength.

$$\boxed{\varepsilon_{rms} = \sqrt{\det \sigma} = \sqrt{\sigma_{11}\sigma_{22} - \sigma_{12}^2}} \qquad (2)$$

Exercise L3: In a transport line for p = 7.5 GeV/c protons are two measurement stations. The first is located exactly in the waist of the beam and shows a beam width of σ_y = 3 mm, the second at a distance of s = 10 m shows a width of σ_y = 9 mm. Assuming no optical elements in this part, calculate the emittance and the normalized emittance of the beam.

No optical elements => $M = \begin{pmatrix} M_{11} & M_{12} \\ M_{21} & M_{22} \end{pmatrix} = \begin{pmatrix} 1 & s \\ 0 & 1 \end{pmatrix}$ (3)

Waist => $\alpha = \sigma_{12} = \sigma_{21} = 0$ $\left(= -\frac{1}{2}\cdot\frac{d\beta}{ds}\right)$ $\left(\varepsilon_{rms} = \sqrt{\sigma_{11}\sigma_{22} - \sigma_{12}^2} = \sqrt{\sigma_{11}\sigma_{22}}\right)$ (4)

Momentum p = 7.5 GeV/c => relativistic $\gamma\beta \approx 7.5$

Measured width at s = 0 => $(3\text{ mm})^2 = \sigma_y^2(0) = \sigma_{11}$ (5)

Calculate σ_{22} with width measured at s = 10 m and with (1 and α=0) =>

$(9\text{ mm})^2 = \sigma_y^2(10) = M_{11}^2\sigma_{11} + M_{12}^2\sigma_{22} = \sigma_{11} + s^2\sigma_{22}$ (σ_{11} and σ_{22} at s=0) (6)

with (5) => $\sigma_{22} = \dfrac{\sigma_y^2(10) - \sigma_y^2(0)}{s^2}$ (7)

With (4) and (7) =>

$$\varepsilon_{rms} = \sqrt{\sigma_{11}\sigma_{22}} = \sqrt{\sigma_y^2(0)\cdot\frac{\sigma_y^2(10) - \sigma_y^2(0)}{s^2}} = \frac{\sigma_y(0)}{s}\sqrt{\sigma_y^2(10) - \sigma_y^2(0)}$$

ε_{rms} = 2.5 · 10^{-6} π m rad or $\varepsilon^{normalized} = \varepsilon_{rms}\,\gamma\,\beta$ = 19 · 10^{-6} π m rad = 19 π mm mrad

---

ε_{rms} = 2.5 · 10-6 π m rad or

$\varepsilon_{normalized} = \varepsilon_{rms}\,\gamma\,\beta$ = 19 · 10-6 π m rad = 19 π mm mrad

Additional exercise: Calculate β(s=0 and s=10m)

Beam width $\sigma_{rms} = \sqrt{\beta(s)\cdot\varepsilon}$

At s=10 m: $\sigma^2 = \beta\varepsilon$ => β = 32.4 m

At s= 0 m : β = 3.6 m

Still more:

What is the influence on the emittance ε assuming at s = 10m this β, a dispersion of D = 1 m and a momentum spread of $\Delta p/p = 10^{-3}$?

$$\varepsilon = \frac{\sigma^2 - \left(D\cdot\frac{\Delta p}{p}\right)^2}{\beta} = \frac{81\cdot10^{-6} - 1\cdot10^{-6}}{32.4} = 2.469\,\pi\,mm\,mrad$$

or ≈1% which is less than the typical accuracy of a profile measurement

---

End of emittance calculations, let's go to some instruments

Resolution

The overall resolution is limited by: Depth of Field, Camera (H and V) and lens resolution. Phosphor screen grain size, air waves and mechanical vibration, a factor in measuring beams of tens of micron size, are not significant for beam sizes in the Millimeter range.

Depth of field is a factor because the screen is tilted at 45° with the top at a different distance from the lens than the bottom. This matters if the beam is well off center or large. In the latter case, however, finer resolution isn't required.

Camera resolution is limited by the number of pixels in the array and the readout electronics bandwidth. The overall resolution can be calculated using the manufacturer's data for the cameras and lenses and the parameters of the beam and optical path for each location.

Ref:
Design of the Beam Profile Monitor System for the RHIC Injection Line *
R. L. Witkover
PAC95
http://accelconf.web.cern.ch/AccelConf/p95/ARTICLES/TPB/TPB26.PDF

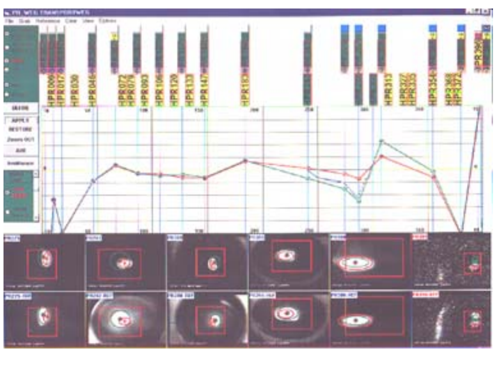

That’s the end of the screen session